

MECHANICAL BEHAVIOUR OF SPHERIODAL GRAPHITE CAST IRON IN THE TEMPERATURE RANGE BETWEEN -100°C AND $+100^{\circ}\text{C}$

V.E. FIERRO^{†‡}, J.A. SIKORA^{*}, A.F. ANSALDI[†], P.J.J. RATTO[†],
F.R. AGÜERA^{†‡} and H.N. ALVAREZ VILLAR^{†‡}

[†]CITEFA, Dpto. Ciencia y Técnica de Materiales, Juan Bautista de Lasalle 4397, (1603) Bs. As., Argentina
pratto@citefa.gov.ar

[‡]Universidad de la Marina Mercante, UdeMM, Rivadavia 2258, (1034) Cap. Fed., Argentina

^{*}INTEMA, Fac. de Ing., Univ. Nac. de Mar del Plata, Av. Juan B. Justo 4302, (7600) Mar del Plata, Argentina

Abstract— Impact tests were done on spheroidal graphite cast iron samples, with five different microstructures. These were obtained by means of the following heat treatments: subcritical annealing, normalizing and two different austempering processes. Other samples were tested in their as-cast condition. The tests were carried out in a temperature range from -100°C to $+100^{\circ}\text{C}$. Also, tensile tests and hardness measurements were performed to qualify the samples. Every specimen came from a single melt, cast in “Y” blocks of two different thicknesses. The impact test results showed an alteration in the fracture behaviour as a function of temperature. The transition temperature, in particular, showed a meaningful shift with the enlargement of the “Y” block. This feature can lead to lower performances than expected. The harder and tougher the matrix, the more important this shift was.

Keywords— Cast iron, ADI, low temperature impact properties.

I. INTRODUCTION

For many years, the ADI (Austempered Ductile Iron) has been considered as an alternative material, substitute for steel in several mechanical components, because it offers the possibility of obtaining a broad range of mechanical properties starting from a generic spheroidal graphite cast iron melt and applying specific heat treatments.

Also, it has a lower manufacturing cost and the capacity of obtaining complex shape components as it is a cast material. Nevertheless, it is a relatively new material, so several of its properties are at present subject of study or are still unknown.

In the bibliography there are few reports about the low temperature behaviour of ADI (Lunyendijk and Nieswaag, 1983; Dorazil and Holzmann, 1991).

The aim of this paper is to characterize the impact response of two different ADI grades and to compare them with the response of the other matrices (pearlitic and ferritic) obtained from the same industrial melt, in the range between -100°C and $+100^{\circ}\text{C}$. Also, a comparison between specimens obtained from two different thickness cast blocks was done.

II. EXPERIMENTAL PROCEDURE

Two “Y” blocks (ASTM A 536-84) of 13 mm and 75 mm in thickness were cast in green sand molds. The chemical composition of the melt was slightly alloyed (Table 1). Samples for Charpy impact tests and for tensile tests were machined from the blocks. A total of 380 unnotched Charpy specimens of 10X10X55 mm (ASTM A 327M-91) and 30 tensile test specimens 6 mm in diameter (ASTM A 897M-90) were performed.

Table 1. Chemical composition of the melt (wt. %).

C	Si	Mn	S	P	Mo	Cu	Mg
3.45	3.22	0.27	0.014	0.03	0.03	0.07	0.045

To avoid troubles with the heat treatment penetration reported in the literature (Hayrynen *et al.*, 1989; Faubert *et al.*, 1990; Faubert *et al.*, 1991) the samples were heated after the machining. Table 2 describes the codification used and the heat treatment parameters for every batch of specimens. Nodule count, nodule size and nodularity were determined (ASTM A 247-67) on metallographic samples in their as-cast condition (Table 3).

Table 2. Heat treatments, variables and microstructures.

Set code	"Y" Block size	Treatment	Austenitizing temperature and time	Austempering temperature and time	Matrix
AC	13mm	As-cast	-----	-----	Ferritic
AG	75mm				
PC	13mm	Normalizing	890 °C / 60 min.	-----	Pearlitic
PG	75mm				
FC	13mm	Annealing	680 °C / 36 h	-----	Ferritic
FG	75mm				
ADI 1C	13mm	Austempering	900 °C / 60 min	370 °C / 60 min	ADI
ADI 1G	75mm				
ADI 2C	13mm	Austempering	915 °C / 60 min	280 °C / 90 min	ADI
ADI 2G	75mm				

The tensile tests were done on an MTS 810 universal machine at room temperature (ASTM E 8M-90a). The Charpy impact tests were done in a Shimadzu pendulum of 300 J maximum capacity, with unnotched specimens (ASTM A 897M-90 and ASTM A 327M-91). Rockwell hardness was determined as the mean over 5 measurements.

Table 3. Microstructural characteristics.

Set Code	"Y" block size	Nodule Count [n/mm ²]	Nodule Size	Nodularity [%]
AC	13mm	240	5/6	>95
AG	75mm	98	4	>90

Charpy specimens were cooled in a bath with ethyl alcohol and dry ice for temperatures down to -60°C, and with ethyl alcohol and liquid nitrogen spray for reaching -100°C. The tests at temperature above the room temperature were

done using an MTS 651 environmental chamber to heat the specimens.

Temperatures of the bath and the samples were measured and controlled with thermocouples, respecting the maximum time between extracting the specimen from the bath and the test as indicated in the literature (Nastad *et al.*, 1990).

The fractographic analysis was made by environmental scanning electronic microscopy (ESEM) and by optical microscopy with oblique illumination.

III. RESULTS

The results for tensile tests and hardness measurements at room temperature appear in Table 4. These results characterize the mechanical strength of the castings. In the case of the ADI samples, they also allow qualification according to the ASTM A 897M-90 standard.

Table 4. Mechanical properties at room temperature (mean values) and impact results.

Set code	Yield strength 0.2% [MPa]	U.T.S [MPa]	Deformation [%]	Rockwell Hardness	E _U [J]	E _L [J]	T _T [°C]	qw [°C]
AC	420	568	18.0	HRB 90	106	18	-11	11
AG	418	569	15.9	HRB 86	119	14	20	9
FC	392	536	16.4	HRB 86	133	10	-14	15
FG	343	501	15.7	HRB 86	134	13	14	6
PC	764	1068	4.3	HRB 29	62	13	4	32
PG	710	1051	4.1	HRB 28	62	11	36	31
ADI 1C	912	1183	11.5	HRC 36	131	5	-50	38
ADI 1G	866	1062	11.1	HRC 34	109	11	-11	36
ADI 2C	1251	1595	4.8	HRC 45	67	0*	-101	50*
ADI 2G	1213	1587	3.2	HRC 42	90	0*	8	89

*Values constrained to E_L > 0.

An Oldfield type semiempirical equation (Oldfield, 1975) was used to fit the plot for the experimental data of the Charpy impact test:

$$E(T) = E_U + \frac{(E_L - E_U)}{1 + \exp((T - T_T)/qw)} \quad (1)$$

where: E_U = upper shelf energy; E_L = lower shelf energy; T_T = transition temperature defined as the

mean energy level between E_U and E_L ; qw = a quarter of the length in temperature of the transition range (Table 4). The experimental values for the impact energy vs. temperature for two batches of samples are shown in Fig. 1, with the corresponding fitting curves. In Fig. 2 only the fitting curves are plotted, without the experimental data, for every “Y” block size and matrix type to allow an easier comparison.

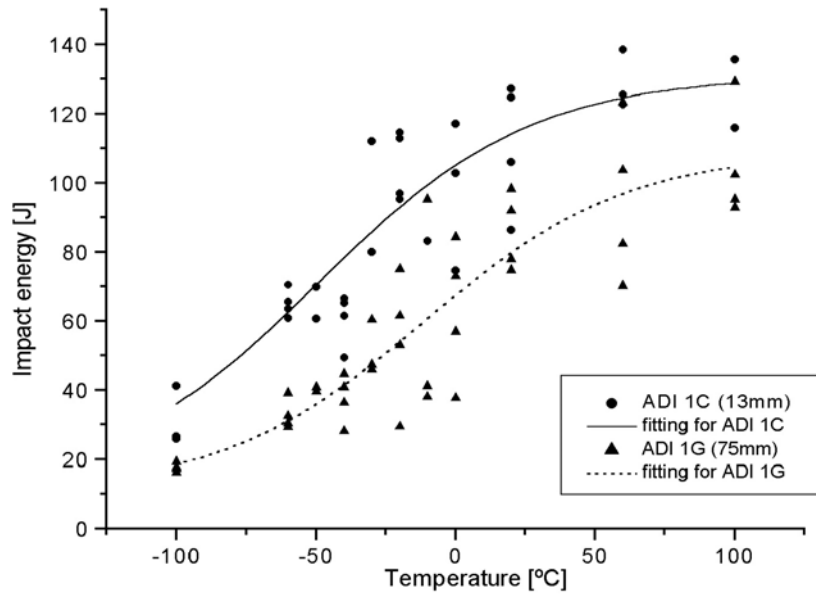


Figure 1. Experimental data and fitting curves of impact energy vs. test temperature for ADI 1 matrix specimens obtained from “Y” blocks of 13mm and 75mm in thickness.

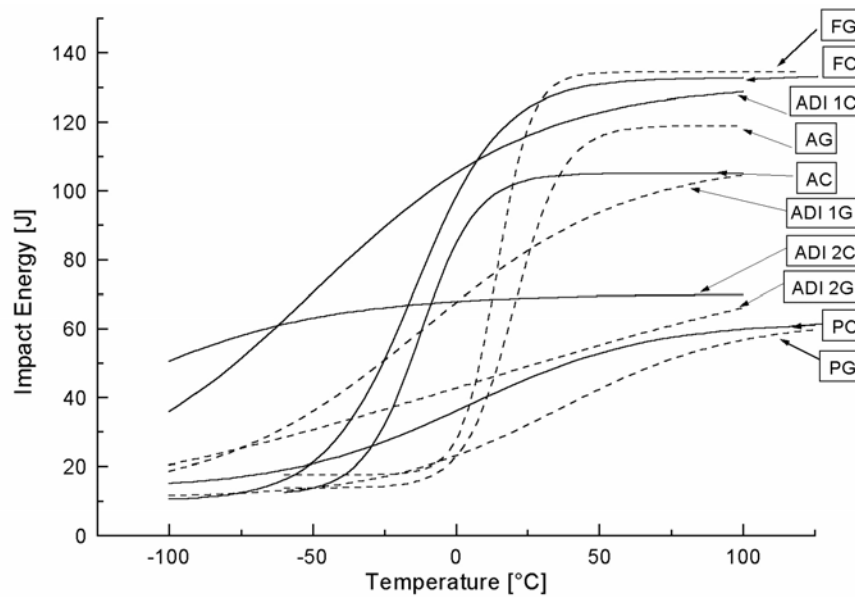


Figure 2. Fitting curves for impact energy vs. test temperature. Comparison between the different matrices obtained from the 13mm and 75mm “Y” blocks.

IV. DISCUSSION

The fitting for the experimental data was truly satisfactory, except for the ADI 2 batch of samples. It allowed the determination of transition temperatures and upper and lower shelf energies (Table 4).

It is observed in the as-cast, ferritic and pearlitic matrices that there is a well defined upper and a lower shelf that do not change with the enlargement of the “Y” block. But the transition temperatures (that are relatively high due to the high silicon content) do raise with this increase of the block size. This fact has been previously reported by Komatsu *et al.* (1994) for fracturemechanic tests done on ferritic samples.

The ADI samples obtained from 13mm thickness “Y” blocks show an impact response consequent with the results reported by Dorazil and Holzmann (1991) and Luyendijk and Nieswaag (1983).

For the ADI 1 samples, the upper and lower shelf energies cannot be correctly determined in this temperature range, although a 50°C shift in the transition temperature can be estimated. This shift indicates a limitation in the material specifications for the big size “Y” block specimens because qualifies as 1050/700/7 ASTM A 879M-90 ADI grade 2. This grade requires an 80 Joules impact response.

The ADI 2 samples show a smoother transition than the other matrices. The upper shelf energy is the same for both 13mm and 75mm “Y” block sizes within the uncertainty due to the high dispersion in the measurements. The samples obtained from the small “Y” blocks do not show a fall in the impact energy until -100°C . The samples obtained from the big “Y” blocks show a smooth fall for temperatures below 0°C .

An estimate calculation could be done only for the big “Y” blocks with the constraint $E_L > 0$. The result is a minimum shift of 60°C in the transition temperature. Again, the samples obtained from the big “Y” blocks show a worse response than those obtained from the small “Y” blocks, although both of them qualify as 1400/1100/1 ASTM A 879M-90 ADI grade 4.

The fractographic analysis shows a change in the main fracture mode in the matrix for the as-cast and ferritic samples. As the temperature increases, the fracture mode changes from cleavage (brittle) to microvoid coalescence (ductile). The fracture surface shows a large number of nodules in the zone where the microvoid coalescence is more important, even the color of that surface turns to black (in a macroscopic view). The cleavage zone shows its typical appearance, with a lower (apparent) nodule density.

For the ADI 1 samples, a mixed fracture mode is observed in the whole range of temperatures. The ratio between the areas spanned by the microvoid coalescence and the quasicleavage mechanisms increases as the temperature raises (Fig. 3a). In some cases, the microvoid coalescence can span the entire space between the nodules (Fig. 3b). The impact energy value is highest in those cases. Similar mechanisms are observed in the ADI 2 samples, but with a lower microplasticity and microvoid coalescence. This is in agreement with other authors (Fan and Smallman, 1994; Voigt, 1983).

For the ferritic and as-cast samples, a transition between the coalescence and the cleavage zone is clearly observed in several samples instead of a mixed fracture mode. The fact that the crack begins in the coalescence zone and then turns to a cleavage mode is related to the change in the deformation rate during the breaking of the Charpy specimens (Fig. 4a). In agreement with Eldoky and Voigt (1985) it can be explained the initial coalescence zone due to the rounding and arrest of the fissure front produced by the nodules. This mechanism gives rise to the fracture surface appearance.

The pearlitic matrix samples show quasicleavage in the whole range of temperature, as it is shown in Fig. 4b.

The impact energies measured arise fundamentally from the matrix toughness. It is affected by the test temperature and the “Y” block size. The difference between the block sizes has a greater importance for the ADI samples due to the fracture mechanism described and the greater shift in the transition temperature.

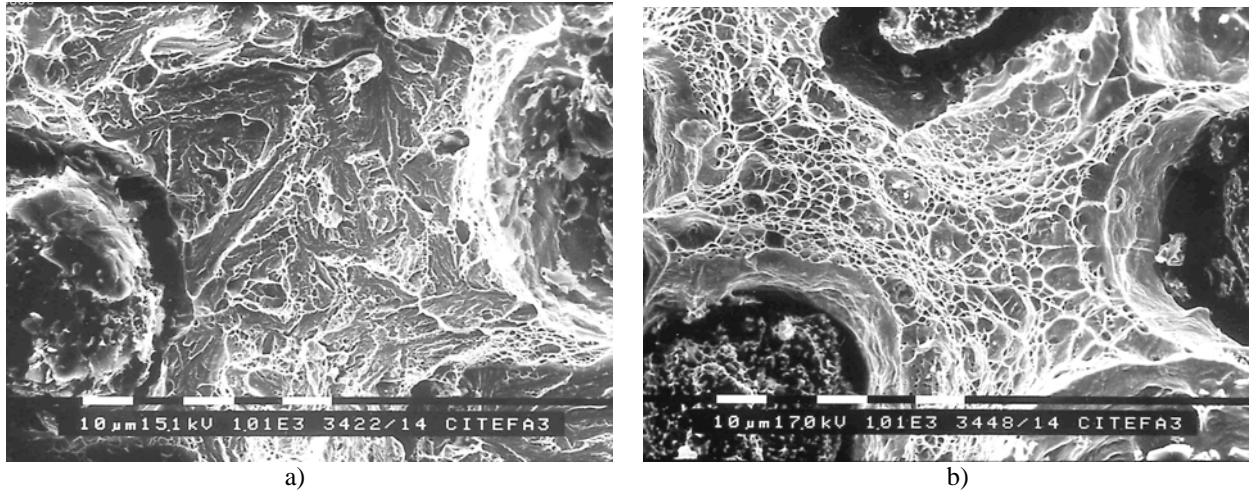


Figure 3. a) Typical fracture surface for an ADI 1 sample tested at low temperature (0°C). A mixed fracture mode is observed: microvoid coalescence near the nodules and quasicleavage in the matrix between them (SEM, X1000). b) Typical fracture surface of ADI 1 sample tested at high temperature (+100°C). The matrix between the nodules shows predominantly the microvoid coalescence as the fracture mode (SEM, X1000).

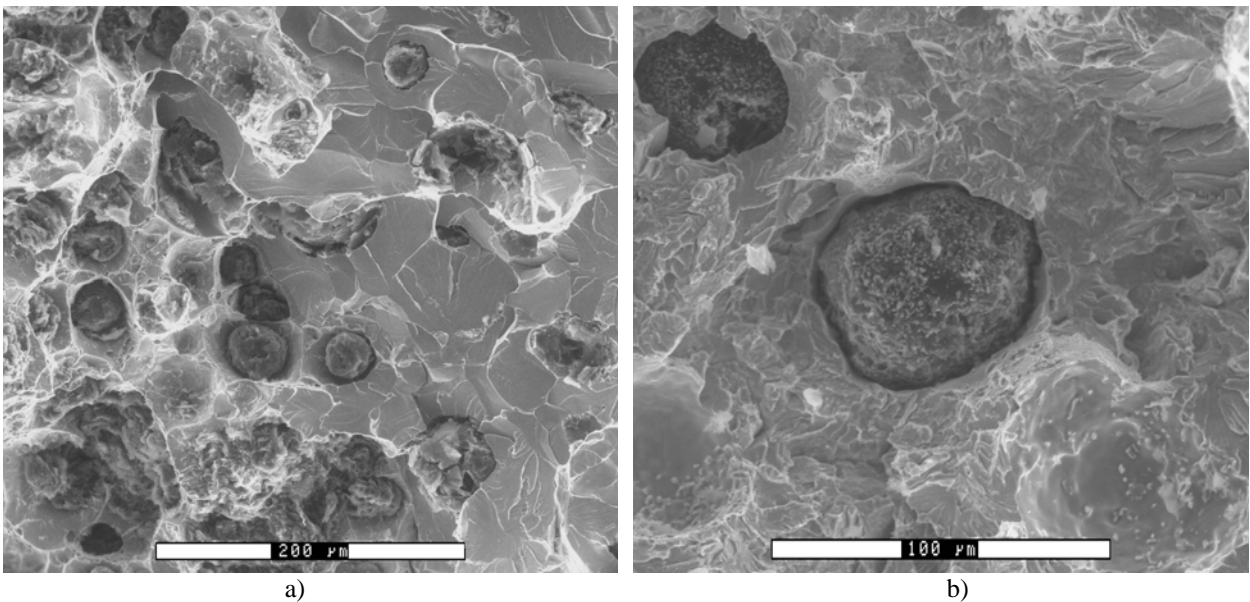


Figure 4. a) Fractography obtained in a ferritic matrix sample. The ductile (on the left) – brittle (on the right) transition is observed. The same behaviour is observed for the as-cast samples (ESEM, X230). b) Typical fractography obtained from a pearlitic matrix sample. A total lack of microvoid coalescence is observed. The fracture mechanism is quasicleavage (ESEM, X500).

V. CONCLUSIONS

The behaviour of the samples is correctly represented by the Eqn. (1) used to fit the Charpy impact energy results. The upper and lower shelf energies and the span in temperatures for the transition zone are not so sensitive to changes in the “Y” block size for every matrix studied. Nevertheless, the transition temperature shows a significant shift according to

the enlargement of the block size. This can lead to a worse response than the one expected for the low temperature range and even for room temperature. The curves obtained show that this shift is greater as the matrix becomes harder and tougher. The whole set of parameters for the ADI samples cannot be precisely determined, but their behaviours are qualitatively similar. The ADI samples show particular fracture mechanisms that distinguish them from the other

spheroidal graphite cast iron samples, and account for the greater shift in the transition temperature.

ACKNOWLEDGEMENTS

This paper was supported by Agencia Nacional de Promoción Científica y Tecnológica, PICT 97/02156.

The authors wish to thank the collaboration given by INTEMA, The UdeMM foundation and CITEFA's Prototype Department. We also thank C. Sommers, A. Reynoso, M. Giordano, A. Graus, R. Gastien, A. Fernández and R. Morris for their assistance.

REFERENCES

- ASM Specialty Handbook, *Cast iron*, Editor J. R. Davis, 1st edition, ASM International, Ohio, 356-392 (1996).
- Dorazil, E. and M. Holzmann, "Fracture behaviour of austempered ductile iron", *Proc. World Conf. on ADI*, Bloomington, IL, AFS, Des Plaine, March, 32-66 (1991).
- Eldoky, L. and R.C. Voigt, "Fracture of ferritic ductile cast iron", *AFS Transactions*, **93**, 621-630 (1985).
- Fan, Z.K. and R.E. Smallman, "Some observations on the fracture of austempered ductile iron", *Scripta Metallurgica et Materialia*, **31** (2), 137-142 (1994).
- Faubert, G., D. Moore and K. Rundman, "Heavy section ADI: tensile properties in as-cast and austempered condition", *AFS Transactions*, **99**, 551-561 (1991).
- Faubert, G., D. Moore and K. Rundman, "Heavy section ADI: tensile properties in as-cast and austempered specimens", *AFS Transactions*, **98**, 831-843 (1990).
- Hayrynen, K., G. Faubert, D. Moore and K. Rundman, "Heavy section ADI: microsegregation, microstructure and tensile properties", *AFS Transactions*, **97**, 747-756 (1989).
- Komatsu, S., T. Shiota, T. Matsuoka and K. Nakamura, "Effects of several main factors on ductile-brittle transition behaviour of fracture toughness in SG cast iron", *AFS Transactions*, **102**, 121-125 (1994).
- Lunydijk, T. and H. Nieswaag, "The influence of silicon on the toughness of bainitic ductile iron", *50th International Foundry Congress*, Cairo, 102-114 (1983).
- Metals Handbook, *Microstructure of cast iron*, Vol. 7, Editor G. E. Dieter, 8th edition, ASM International, Ohio, 81-100 (1972).
- Nastad, R., R. Swain and R. Berggren, "Influence of Thermal Conditioning Media on Charpy Specimen Test Temperature", *Charpy Impact Test: Factors and Variables (STP 1072)*, Editor J. M. Holt, ASTM, Chelsea, 195-210 (1990).
- Oldfield, W., "Curve fitting impact test data: a statistical procedure", *ASTM Standardization News*, November, 24-29 (1975).
- Voigt, R.C. and L.M. Eldoky, "Crack initiation and propagation in as-cast and fully pearlitic ductile cast irons", *AFS Transactions*, **94**, 637-644 (1986).
- Voigt, R.C., "Microstructural analysis of austempered ductile cast iron using the scanning electron microscope", *AFS Transactions*, **91**, 253-262 (1983).